

The following article appeared in Journal of Maps 15(2): 8-18 (2018); and may be found at: <https://doi.org/10.1080/17445647.2018.1531075>

This is an open access article distributed under the Creative Commons Attribution 4.0 International (CC BY 4.0) license <https://creativecommons.org/licenses/by/4.0/>



## Geology of the late Pliocene – Pleistocene Acoculco caldera complex, eastern Trans-Mexican Volcanic Belt (México)

Denis Ramón Avellán, José Luis Macías, Paul W. Layer, Guillermo Cisneros, Juan Manuel Sánchez-Núñez, Martha Gabriela Gómez-Vasconcelos, Antonio Pola, Giovanni Sosa-Ceballos, Felipe García-Tenorio, Gabriela Reyes Agustín, Susana Osorio-Ocampo, Laura García-Sánchez, Irma Fabiola Mendiola, Joan Marti, Héctor López-Loera & Jeff Benowitz

To cite this article: Denis Ramón Avellán, José Luis Macías, Paul W. Layer, Guillermo Cisneros, Juan Manuel Sánchez-Núñez, Martha Gabriela Gómez-Vasconcelos, Antonio Pola, Giovanni Sosa-Ceballos, Felipe García-Tenorio, Gabriela Reyes Agustín, Susana Osorio-Ocampo, Laura García-Sánchez, Irma Fabiola Mendiola, Joan Marti, Héctor López-Loera & Jeff Benowitz (2019) Geology of the late Pliocene – Pleistocene Acoculco caldera complex, eastern Trans-Mexican Volcanic Belt (México), Journal of Maps, 15:2, 8-18, DOI: [10.1080/17445647.2018.1531075](https://doi.org/10.1080/17445647.2018.1531075)

To link to this article: <https://doi.org/10.1080/17445647.2018.1531075>



© 2018 The Author(s). Published by Informa UK Limited, trading as Taylor & Francis Group on behalf of Journal of Maps



[View supplementary material](#)



Published online: 19 Nov 2018.



[Submit your article to this journal](#)



Article views: 674



[View Crossmark data](#)



## Geology of the late Pliocene – Pleistocene Aocolco caldera complex, eastern Trans-Mexican Volcanic Belt (México)

Denis Ramón Avellán<sup>a</sup>, José Luis Macías<sup>b</sup>, Paul W. Layer<sup>c</sup>, Guillermo Cisneros<sup>b</sup>, Juan Manuel Sánchez-Núñez<sup>d</sup>, Martha Gabriela Gómez-Vasconcelos<sup>b</sup>, Antonio Pola<sup>e</sup>, Giovanni Sosa-Ceballos<sup>b</sup>, Felipe García-Tenorio<sup>b</sup>, Gabriela Reyes Agustín<sup>b</sup>, Susana Osorio-Ocampo<sup>f</sup>, Laura García-Sánchez<sup>f</sup>, Irma Fabiola Mendiola<sup>b</sup>, Joan Martí<sup>g</sup>, Héctor López-Loera<sup>e,h</sup> and Jeff Benowitz<sup>c</sup>

<sup>a</sup>Cátedras CONACYT – Instituto de Geofísica, Universidad Nacional Autónoma de México, Morelia, Mexico; <sup>b</sup>Instituto de Geofísica, Universidad Nacional Autónoma de México, Morelia, Mexico; <sup>c</sup>College of Natural Science and Mathematics, University of Alaska at Fairbanks, Fairbanks, AK, USA; <sup>d</sup>Instituto Politécnico Nacional-CIEMAD, Ciudad de México, Mexico; <sup>e</sup>Escuela Nacional de Estudios Superiores, Universidad Nacional Autónoma de México, Morelia, Mexico; <sup>f</sup>Posgrado en Ciencias de la Tierra, Instituto de Geofísica, Universidad Nacional Autónoma de México, Morelia, Mexico; <sup>g</sup>Instituto de Ciencias de la Tierra Jaime Almera, CSIC, Barcelona, Spain; <sup>h</sup>División de Geociencias Aplicadas, Instituto Potosino de Investigación Científica y Tecnológica A.C., San Luis Potosí, Mexico

### ABSTRACT

We present a new 1:80,000-scale geologic map of the Aocolco caldera (Ac) located between the states of Puebla and Hidalgo in eastern México. The map, encompassing an area of 856 km<sup>2</sup>, is grounded on an ArcMap data set and is supported by nine new <sup>40</sup>Ar/<sup>39</sup>Ar dates. The caldera lies upon Cretaceous limestones and Miocene to Pliocene volcanic rocks (13–3 Ma). The caldera consists of 31 lithostratigraphic units formed between 2.7 and 0.06 Ma that include a wide variety of volcanic landforms (cinder cones, lava domes). The caldera has a semi-circular shape (18–16 km) bounded by the Atotonilco scarp to the north, the NW–SE Manzanito fault to the west, and scattered vents to the east and southern parts. The distribution of the Aocolco ignimbrite, the lithic breccia, and lacustrine sediments define the caldera ring fault. Late Pleistocene activity and pervasive hydrothermal alteration suggest a high geothermal potential in the area.

### ARTICLE HISTORY

Received 25 April 2018  
Accepted 26 September 2018

### KEYWORDS

Geology; volcanic stratigraphy; Aocolco caldera complex; Puebla

## 1. Introduction

The Aocolco caldera is located in the states of Puebla and Hidalgo in eastern México (Figure 1). The caldera has been an area of interest for geothermal exploration by the National Power Company (Comisión Federal de Electricidad = CFE). Renewed interest in the geothermal potential for the caldera by the Centro Mexicano de Innovación en Energía Geotérmica (CeMIE Geo) supported detailed field mapping and <sup>40</sup>Ar/<sup>39</sup>Ar geochronology, presented in this geologic map, and whole-rock, isotopic, and mineral chemistry of these rocks (Sosa-Ceballos, Macías, Avellán, Salazar-Hernenegildo & Boijseauneau-López, 2018). This new map improves upon earlier regional mapping (De la Cruz-Martínez & Castillo-Hernández, 1986) and detailed volcanological, hydrothermal, and geochronologic investigations (López-Hernández & Castillo-Hernández, 1997; López-Hernández et al., 2009; López-Hernández & Martínez, 1996). López-Hernández et al. (2009) concluded that the Aocolco caldera is nested within the 32-km wide Tulancingo caldera (~3.0 to 2.7 Ma). However, we did not find any evidence in the study area for the existence of the larger Tulancingo caldera.

Therefore, in this contribution we focus on the description of the evident Aocolco caldera that generated an andesitic ignimbrite and subsequent volcanism described as the Aocolco caldera complex (Acc). Here, we propose a new edge of the Aocolco caldera (18 × 16 km wide) based upon our new cartography of the ignimbrite, the lithic lag breccia associated, and the location of intra-caldera lacustrine sediments.

## 2. Study area

The Acc is located at the eastern sector of the Trans-Mexican Volcanic Belt (TMVB). The TMVB is directly linked to the subduction of the Rivera and Cocos plates beneath the North American plate along the Middle-American Trench (e.g. Demant, 1978) (Figure 1(A)). The TMVB is a ca. 1000-km long arc with a transverse ~E–W orientation that extends from Nayarit state (to the west) to Veracruz state (to the east). The Cocos slab beneath the Aocolco region lies at depths between 260 and 320 km; and the crustal thickness is between 45 and 50 km (Urrutia-Fucugauchi & Flores-Ruiz, 1996). The Ac rocks in the area are deformed by

**CONTACT** Denis Ramón Avellán ✉ [denisavellan@gmail.com](mailto:denisavellan@gmail.com) 📍 Cátedras CONACYT – Instituto de Geofísica, Universidad Nacional Autónoma de México, Antigua Carretera a Pátzcuaro 8701, 58190 Morelia, Michoacán, Mexico

© 2018 The Author(s). Published by Informa UK Limited, trading as Taylor & Francis Group on behalf of Journal of Maps

This is an Open Access article distributed under the terms of the Creative Commons Attribution License (<http://creativecommons.org/licenses/by/4.0/>), which permits unrestricted use, distribution, and reproduction in any medium, provided the original work is properly cited.

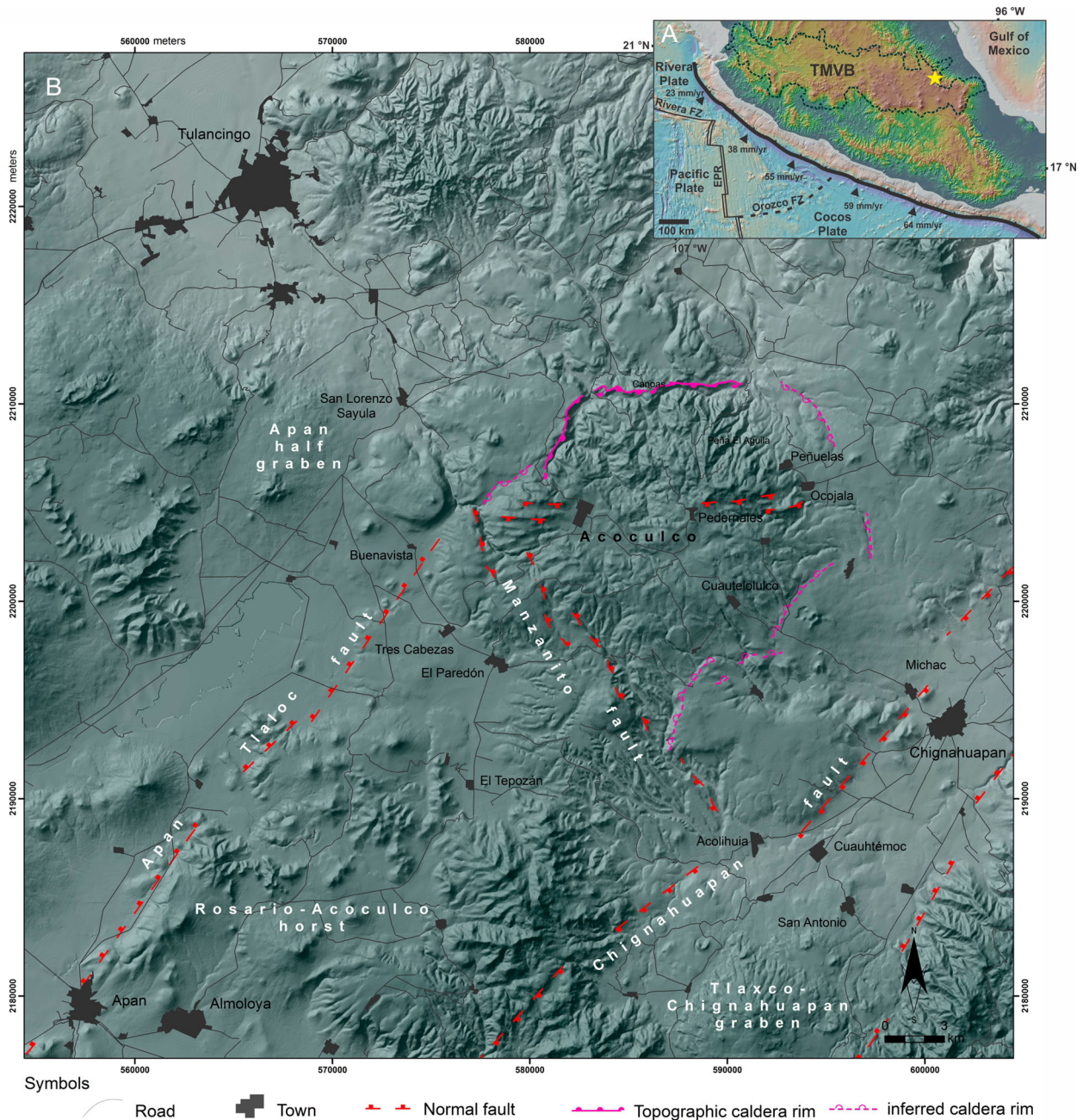


**Figure 1.** (A) Regional tectonic regime of Central Mexico that shows the active subduction of the Rivera and Cocos Plates beneath the North American Plate at the Middle-American Trench, and distribution of the Trans-Mexican Volcanic Belt (TMVB). The shaded relief map and bathymetric data were acquired and modified from [Ryan et al. \(2009\)](#). The yellow star shows the location of the Acc. (B) Shaded relief map showing the Acc, regional faults systems and main villages in the region. The Manzanito fault belongs to the Tulancingo-Tlaxco fault system, and the Apan-Tlaloc and Chignahuapan faults belong to the Tenochtitlán-Apan fault system.

three main fault systems: the NE-striking Tenochtitlán-Apan fault system, and the NW-striking Tulancingo-Tlaxco fault system ([Figure 1\(B\)](#)). Locally, the Tenochtitlán-Apan fault system is represented by the Apan-Tlaloc and Chignahuapan faults, and the Tulancingo-Tlaxco fault system is represented by the Manzanito fault. The NE- and NW-striking normal fault systems intersect each other ([Campos-Enríquez, Alatríguez-Vilchis, HuizarÁlvarez, Marines-Campos, & Alatorre-Zamora, 2003; Lermo, Antayhua, Bernal, Venegas, & Arredondo, 2009](#)), creating an orthogonal arrangement of grabens, half-grabens and horsts. The Acoculco

caldera is located on the NE–SW Rosario-Acoculco horst ([García-Palomo et al., 2017; García-Palomo, Macías, Tolson, Valdez, & Mora, 2002](#)), which is delimited to the west by the 235°-striking and NW-dipping Apan-Tlaloc fault ([Huizar-Álvarez, Campos-Enríquez, Lermo-Samaniego, Delgado-Rodríguez, & Huidobro-González, 1997; Mooser & Ramírez, 1987](#)) and to the east by the 55°-striking and SE-dipping Chignahuapan fault. The Acoculco caldera rests upon sedimentary marine Cretaceous limestones of the Sierra Madre Oriental ([López-Hernández et al., 2009](#)), and Miocene volcanic rocks belonging to early

stages of the TMVB (García-Palomo et al., 2002). The Cretaceous limestones do not crop out inside the Aco-culco caldera but were cut in the geothermal exploration drill-holes of CFE, from 800 to 1200 m of depth in well EAC1, and from 350 to 450 m of depth in well EAC-2 (López-Hernández et al., 2009; Viggiano-Guerra, Flores-Armenta, & Ramírez-Silva, 2011). Limestones with chert bands are exposed to the east of the town of Chignahuapan. The Aco-culco caldera succession is also interbedded with deposits of the Apan-Tezontepec Volcanic Field (ATVF) that consists of 280 scoria cones, 10 shield volcanoes, and 5 domes (García-Palomo et al., 2002). Most volcanoes are made of basaltic andesitic lavas with phenocrysts of olivine and plagioclase, and dacitic domes. The age of the ATVF spans from at least  $2.25 \pm 0.04$  Ma to the Holocene (García-Tovar et al., 2015).

### 3. Methods

New geological data coupled with previously published geological information were combined to obtain the new Acc geological map scale 1:80,000. This geological information was overlapped on a 3D surface map compiled with a 15-m resolution Digital Elevation Model (DEM) from INEGI (Instituto Nacional de Estadística y Geografía) with  $x$ - $y$ - $z$  coordinates and satellite imagery. The map is georeferenced with respect to the WGS-1984-UTM-Zone-14N coordinate system. We overlapped Landsat 8 (30-m multispectral) and Spot 6 (1.5-m panchromatic and 6-m multispectral) mosaics obtained from the USGS data and ERMEXS (Estación de Recepción México de la Constelación Spot) protected by SEMAR (Secretaría de Marina), and INEGI (Instituto Nacional de Estadística Geografía e Informática) to obtain an orthophoto map scale 1:20 000 (1.5 m-resolution) with ERDAS 9.1. The DEM data was used to construct thematic maps (shaded, slope and altitude) by interpolating points with a 15-m<sup>2</sup>-resolution in ArcMap 10.2. The DEM data, the DEM-shaded relief, and the orthophoto map were imported in ERDAS image 9.1 to generate anaglyphs to visualize surface morphological features, color texture, and vegetation in 3D. This information was used for geomorphological analysis, which consisted in delineating the different types of morphological features such as volcanic structures, lithological contacts, erosion zones, and main faults. Site observations (mapping of contacts, drawing of stratigraphic columns, rock descriptions, and collection of samples) at 128 locations were spatially located using a GPS. Forty samples were collected for petrographic and nine for <sup>40</sup>Ar/<sup>39</sup>Ar geochronological analysis performed at the Geochronology Laboratory at the University of Alaska Fairbanks following the techniques of Benowitz, Layer, and Vanlaningham (2014). The results are quoted to the  $\pm 1$  sigma level and calculated using the constants of Steiger and Jäger (1977).

## 4. Morphology of the caldera

The morphology of the study area revealed that Aco-culco has a medium to high mountain relief with a maximum elevation of 3090 m above sea level (Figure 1(B)). Its surrounding relief is dominated by smooth slopes (<5°) and morphology with hogback and alluvial plains with altitudes that vary between 2690 and 2260 m. Two important features, the Atotonilco and Manzanito structures define the modern topographic rim of the Aco-culco caldera. The Atotonilco scar defines the northern edge of the caldera with a steep scar that bounds inner lava flows, and is the venting site of lava flows that extend to the north. The scarp succession includes the Aco-culco ignimbrite *Ari* and subsequent lava flows and domes (see Section 4). To the west, an NW–SE right-lateral fault limits the western edge of the caldera. Locally, this fault named Manzanito (Figure 1(B) and geologic map) defines the southwestern edge of the caldera rim where the Tecoloquillo ignimbrite and dome were emplaced. Younger deposits mask the eastern and southern parts of the caldera rim, however, the Ailitla lava flow, the Paila lava cone, and the Encimadas ignimbrite point to venting sites along the caldera ring fault (Figure 1(B), and geologic map). These structures define in plain view the 18 × 16 km asymmetric shape of the caldera with an intra-caldera ignimbrite, and uplifted sediments. This shape differs considerably from the nearly circular form proposed by López-Hernández et al. (2009). We have not found any evidence of a larger caldera structure (Tulancingo caldera) that would host the Aco-culco caldera as suggested by López-Hernández et al. (2009).

## 5. Stratigraphy and geological mapping

We present a geological map with 40 lithostratigraphic units, 31 belonging to the Aco-culco caldera complex lumped into pre-caldera, syn-caldera, early post-caldera, and late post-caldera successions (Figure 2). These successions correspond to different phases of the caldera formation and were defined according to their distribution, stratigraphic position, age, and mineral composition. We also described one Miocene unit that represents an early stage of the TMVB and seven units associated to the Apan Tezontepec Volcanic Field (ATVF). The ATVF units are described as extra-caldera volcanism because their origin is not related with the caldera. The location and description of all units is given with respect to the caldera rim (Figure 1(B), and the geologic map).

### 5.1. Pre-caldera

The *Peñuela* dacitic domes (*Pdd*) are elongated in an NW–N direction and exposed south of the caldera rim. *Pdd* consists of pinkish-gray rocks with a mottled

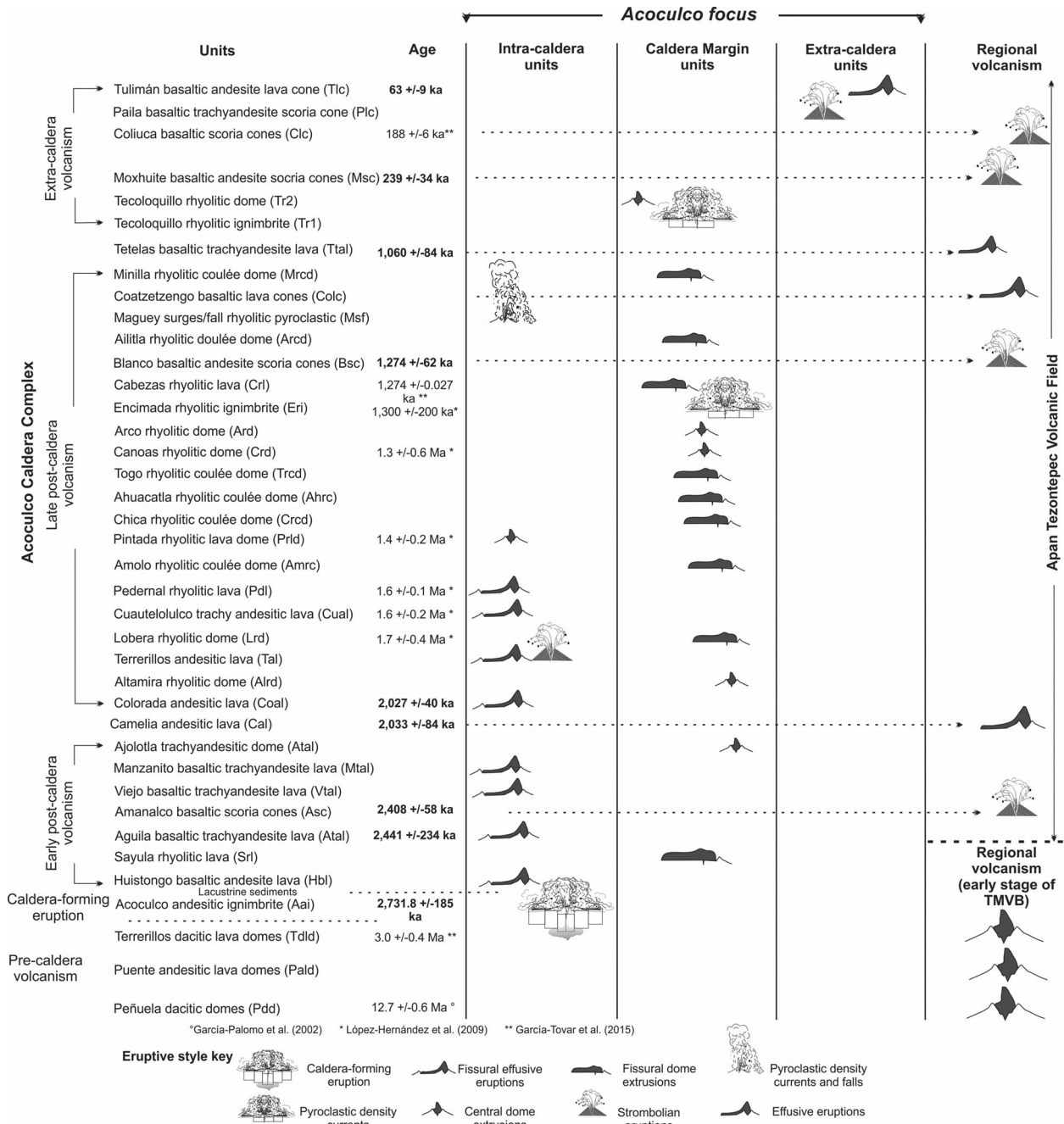


**Figure 2.** Composite stratigraphic section of the volcanic units described in the area that were produced during the early stages of formation of the Trans-Mexican Volcanic Belt (TMVB), the Acoculco caldera and the extra-caldera volcanism related to the ATVF as described in text.

appearance resulting from abundant greenish-gray enclaves (Table 2). García-Palomo et al. (2002) reported a K-Ar whole-rock age of  $12.7 \pm 0.6$  Ma for this rock.

The *Puente andesitic lava domes (Pald)* are exposed to the north of the caldera rim. Pald has a hogback morphology, it is light-gray with greenish-gray enclaves.

The *Terrerillos dacitic lava domes (Tld)* are exposed south of the caldera rim with a hill morphology. López-Hernández et al. (2009) described *Tld* as basalts of the ATVF; however, García-Tovar et al. (2015) described it as dacitic in composition. *Tld* is light-gray in color has rounded columns and a blocky surface. García-Tovar et al. (2015) reported a K-Ar whole-rock age of  $3.0 \pm 0.4$  Ma.

### 5.2. Syn-caldera

The *Acoculco andesitic ignimbrite (Aai)* corresponds to the caldera-forming eruption. The *Aai* unit crops out at the north, west and south inner parts of the Acc. *Aai* consists of unsorted beds of pumice and lithic blocks and lapilli supported by a fine-ash matrix that are interbedded with a heterolithologic co-ignimbritic breccia. This breccia is made of blocks and lapilli of lava, accidental lithics and pumice set in a fine ash matrix. Laterally, this breccia shifts to an unsorted fine ash bed enriched in lapilli pumice and crystals. Pumice is greenish-gray to white with plagioclase phenocrysts, and lava fragments are porphyritic, banded, and

aphanitic, varying from gray to pinkish-gray, with plagioclase and amphibole phenocrysts. A  $^{40}\text{Ar}/^{39}\text{Ar}$  age on plagioclase separates yielded  $2732 \pm 185$  ka for this unit (Table 1).

A sequence of *lacustrine sediments* (*Ls*) is exposed inside the caldera rim in the south, southwest, and northern parts. It consists of an alternating sequence of white clayed laminae, and dark-gray cm-thick, volcanoclastic beds. These beds are made of rounded lava fragments set in a fine-grained matrix. At sites Ac69 and 119, *Ls* overlies the Acoculco ignimbrite (*Aai*), in particular at Ac119, occurs as a yellowish to ochre sequence due to intense hydrothermal alteration (Table 2).

### 5.3. Early post-caldera

The *Huistongo basaltic andesite lava* (*Hbl*) occurs within the north-northwestern portion of the caldera. The rock is gray to greenish-gray with aphanitic texture due to intense weathering (Figure 3(A)). *Hbl* is younger than *Aai* (~2.7 Ma).

The *Sayula rhyolitic lava* (*Srl*) flow is exposed to the northwest of the caldera margin. The tip portion of the flow forms a flat-topped mesa with steep flow terminus. It consists of gray to black-brown banded obsidian lavas with entablature structure at their fronts.

The *Aguila basaltic trachyandesitic lava* (*Atal*) flow is confined within the northeast portion of the caldera and has a gray blocky surface. Hydrothermal alteration has discolored surfaces of joints to yellowish color. The northern flanks of *Atal* are bounded by the caldera margin. It has a  $^{40}\text{Ar}/^{39}\text{Ar}$  whole-rock age of  $2441 \pm 234$  ka (Table 1).

The *basaltic trachyandesite lavas of the Viejo and Manzanito* (*Vtal* and *Mtal*, respectively) are exposed on the east and south-southwest inner parts of the caldera. These rocks are light-gray in color, the base of *Vtal* is not exposed, and *Mtal* directly overlies the Acoculco ignimbrite (Figure 3(B)).

The *Ajolutla trachyandesitic dome* (*Atad*) occurs at the southeastern rim and outside of the caldera. It has a low hogback morphology with NW–SE alignments. *Atad* is a greenish-light-gray massive blocky flow.

### 5.4. Late post-caldera

The *Colorada andesitic lava* (*Coal*) flow is exposed on the southeast inner portion of the caldera with hogback and hill morphologies. *Coal* is black in color and contains dark-gray aphanitic basaltic enclaves. South of the Cruz Colorada village, *Coal* is reddish to yellowish due to intense hydrothermal alteration that formed clay minerals. *Coal* has a  $^{40}\text{Ar}/^{39}\text{Ar}$  whole-rock age of  $2027 \pm 40$  ka (Table 1). A basaltic dike outcropping near the town of Cruz Colorada intrudes *Coal*. The

dike is ca. 2 km long, 100 m-wide, and oriented north-northwest. The rock is dark-gray to light-gray, aphanitic with plagioclase and olivine microphenocrysts.

The *Altamira rhyolitic dome* (*Alrd*) occurs along the southwestern border of the caldera rim (Figure 3(C)). The *Alrd* has an asymmetrical hogback morphology, parallel to the NW–SE orientation of the Manzanito fault. The rock is light-gray to pinkish-gray with diffuse banding. The upper part of *Alrd* has a holohyaline texture slightly devitrified with spherulites.

The *Terrerillos andesitic lava and scoria cone* (*Tal*) are located on the central-south inner portion of the caldera. The lava flow is reddish, massive, with spheroidal weathering and entablature structure. It contains dark-gray to yellowish-ochre, subrounded basaltic aphanitic enclaves. In some sites, it is highly altered with iron sulfide minerals and a silicified matrix. The *Tal* lava flow is covered by a quarried andesitic scoria cone. The cone exposes poorly sorted, proximal scoria fallout beds made of welded dark-reddish scoria ash with spatter bombs. The rock contains subrounded pumice, basaltic lava, quartz, and alkali feldspars xenocrysts.

The *Lobera rhyolitic dome* (*Lrd*) appears at the western margin and to the west of the caldera margin where it covers the Acoculco ignimbrite. The *Lrd* is a pinkish-white asymmetrical dome with blocky surface and an N–S orientation that is cut by the Manzanito fault. López-Hernández et al. (2009) reported a K–Ar whole-rock age for this rock of  $1700 \pm 400$  ka.

The *Cuaatelolulco andesitic lava* (*Cual*) is exposed on the southern inner part of the caldera. *Cual* has a morphology similar to flatirons pointing to the caldera center. It overlays *Aai* and *Coal*. *Cual* is dark-gray with entablature structure and spheroidal weathering structures. López-Hernández et al. (2009) obtained a  $^{40}\text{Ar}/^{39}\text{Ar}$  age of  $1600 \pm 200$  ka for this rock.

The *Pedernal rhyolitic lava* (*Pdl*) is exposed at the inner, central-northern part of the caldera. The *Pdl* has a low topographic relief with a hogback-hill morphology. It consists of pinkish-gray to pinkish-white lava with blocky surface. White hydrothermally altered zones occur in the vicinity of the Pedernal and Acoculco towns (Figure 3(D)). López-Hernández et al. (2009) reported a K–Ar whole-rock age of  $1600 \pm 100$  ka for this lava.

The Amolo rhyolitic coulée (*Amrc*) dome is exposed outside the northeast margin of the caldera with steep sided levées. *Amrc* is pink-white-gray massive lava flow with entablature structure at its front.

The *Pintada rhyolitic lava dome* (*Prld*) is restricted to the inner western part of the caldera. *Prld* has a low topographic relief with E–W aligned hogback morphology. It has a blocky lava surface with a light-gray to pink color. López-Hernández et al. (2009) reported a K–Ar whole-rock age of  $1400 \pm 200$  ka for this unit.

The *Chica, Ahuacatla and Togo* (*Crcd*, *Ahrc*, and *Trcd*) are rhyolitic coulée domes located outside of

**Table 1.** Summary of whole-rock  $^{40}\text{Ar}/^{39}\text{Ar}$  analyses.

Sample	Groups	Unit	Location		Material	Integrated Age (ka)	Plateau Age (ka)	Plateau information	Isochron Age (ka)	Isochron information
			North	West						
Ac65	<i>Extra-caldera</i>	<b>Tlc</b>	2209728	581555	Whole rock	51 ± 9	<b>63 ± 9</b>	Fractions = 5 67.6% of $^{39}\text{Ar}$ rel. MSWD = 0.03	68 ± 20	Init. $^{40}\text{Ar}/^{36}\text{Ar}$ = 293.6 ± 2.6 MSWD = 1.25 Fractions = 8
Ac101	<i>Apan-Tezontepec Volcanic Field</i>	<b>Msc</b>	2207305	596580	Whole rock	230 ± 26	<b>239 ± 34</b>	Fractions = 8 97.6% of $^{39}\text{Ar}$ rel. MSWD = 1.67	427 ± 152	Init. $^{40}\text{Ar}/^{36}\text{Ar}$ = 287.0 ± 7.9 MSWD = 1.46 Fractions = 8
Ac84	<i>Apan-Tezontepec Volcanic Field</i>	<b>Ttal</b>	2189649	596869	Whole rock	1029 ± 9	<b>1060 ± 8</b>	Fractions = 6 88.8% of $^{39}\text{Ar}$ rel. MSWD = 0.97	1068 ± 33	Init. $^{40}\text{Ar}/^{36}\text{Ar}$ = 291.7 ± 15.8 MSWD = 1.19 Fractions = 6
Ac21	<i>Apan-Tezontepec Volcanic Field</i>	<b>Bsc</b>	2187203	586305	Whole rock	1270 ± 68	<b>1274 ± 62</b>	Fractions = 6 91.2% of $^{39}\text{Ar}$ rel. MSWD = 0.53	1164 ± 279	Init. $^{40}\text{Ar}/^{36}\text{Ar}$ = 303.0 ± 21.6 MSWD = 0.80 Fractions = 8
Ac98A	<i>Late post-caldera</i>	<b>Coal</b>	2202522	592368	Whole rock	1996 ± 31	<b>2027 ± 40</b>	Fractions = 7 97.0% of $^{39}\text{Ar}$ rel. MSWD = 1.77	2005 ± 107	Init. $^{40}\text{Ar}/^{36}\text{Ar}$ = 297.5 ± 4.9 MSWD = 1.95 Fractions = 7
Ac19	<i>Apan-Tezontepec Volcanic Field</i>	<b>Cal</b>	2186168	584881	Whole rock	1992 ± 87	<b>2033 ± 84</b>	Fractions = 6 92.7% of $^{39}\text{Ar}$ rel. MSWD = 1.01	1993 ± 97	Init. $^{40}\text{Ar}/^{36}\text{Ar}$ = 296.4 ± 13.4 MSWD = 1.56 Fractions = 8
Ac49	<i>Apan-Tezontepec Volcanic Field</i>	<b>Asc</b>	2193382	599752	Whole rock	2423 ± 64	<b>2408 ± 58</b>	Fractions = 7 97.4% of $^{39}\text{Ar}$ rel. MSWD = 0.84	2290 ± 68	Init. $^{40}\text{Ar}/^{36}\text{Ar}$ = 315.8 ± 13.5 MSWD = 0.70 Fractions = 9
Ac28	<i>Early post-caldera</i>	<b>Atal</b>	2209324	589436	Whole rock	2495 ± 143	<b>2441 ± 234</b>	Fractions = 4 88.7% of $^{39}\text{Ar}$ rel. MSWD = 5.53	2203 ± 117	Init. $^{40}\text{Ar}/^{36}\text{Ar}$ = 296.8 ± 1.0 MSWD = 2.82 Fractions = 8
Ac69	<i>Syn-caldera</i>	<b>Aai</b>	2200645	584104	Plagioclase	2888 ± 195	<b>2732 ± 185</b>	Fractions = 6 91.5% of $^{39}\text{Ar}$ rel. MSWD	2647 ± 174	Init. $^{40}\text{Ar}/^{36}\text{Ar}$ = 314 ± 12 MSWD = 0.53 Fractions = 8

Notes: All ages are quoted to the ±1 -sigma level and calculated using the constants of Steiger and Jäger (1977). Coordinate system: UTM zone 14. Analyses performed at the Geochronology Laboratory of the University of Alaska at Fairbanks, USA.

**Table 2.** Summary of the textural features of the lithostratigraphic units described for the Aocolcalo caldera complex and surrounding areas.

Group	Unit	Province	Acronym	Rock features
Pre-caldera	Peñuela dacitic domes	TMVB	Pdd	Porphyritic with quartz, plagioclase, alkali feldspar, amphibole, pyroxene, and biotite phenocrysts
	Puente andesitic lava domes		Padl	porphyritic with plagioclase and olivine phenocrysts
	Terrerillos dacitic lava domes		Tdld	Porphyritic with quartz, plagioclase, alkali feldspar and amphibole phenocrysts
Syn-caldera	Aocolcalo andesitic ignimbrite	Acc	Aai	Unsorted beds of pumice and lithic blocks and lapilli supported by a fine-ash matrix
	Lacustrine sediments		Ls	Alternating sequence of white clayed laminae, and dark-gray cm-thick, volcanoclastic beds
Early post-caldera	Huistongo basaltic andesite lava	Acc	Hbl	Gray to greenish-gray in hand specimen aphanitic
	Sayula rhyolitic lava	Acc	Srl	Holohyaline textures partially devitrified with light-gray spherulites and lithophysae
	Aguila basaltic trachyandesitic lava	Acc	Atal	Aphanitic, and contains subrounded granite and sandstones xenoliths
	Amanalco basaltic scoria cones	ATVF	Asc	Scoria is aphanitic, dark-gray, poorly vesiculated with plagioclase and olivine micro-phenocrysts.
	Viejo basaltic trachyandesite lavas	Acc	Vtal	Porphyritic rock with plagioclase and pyroxene phenocrysts
	Manzanito basaltic trachyandesite lavas	Acc	Mtal	Porphyritic rock with plagioclase and pyroxene phenocrysts
	Ajolotla trachyandesitic dome	Acc	Atad	Porphyritic with plagioclase, orthopyroxene and clinopyroxene phenocrysts
Late post-caldera	Camelia andesitic lava	ATVF	Cal	Aphanitic with plagioclase and olivine microphenocrysts
	Colorada andesitic lava	Acc	Coal	Porphyritic with plagioclase, amphibole, clinopyroxene and orthopyroxene phenocrysts
	Altamira rhyolitic dome	Acc	Aldr	Porphyritic with alkali feldspar, quartz, orthopyroxene, and amphibole phenocrysts
	Terrerillos andesitic lava and scoria cone	Acc	Tal	Porphyritic lava with plagioclase, olivine and pyroxene phenocrysts
		Acc		Spatter bombs of the scoria cone are light-gray, porphyritic with plagioclase and olivine phenocrysts
	Lobera rhyolitic dome	Acc	Lrd	Porphyritic to vesicular with alkali feldspar, quartz, and amphibole phenocrysts
	Cuautelolulco andesitic lava	Acc	Cual	Porphyritic with plagioclase, clinopyroxene and olivine phenocrysts and subrounded quartz and alkali feldspar xenocrysts
	Pederal rhyolitic lava	Acc	Pdl	Porphyritic with alkali feldspar, plagioclase, quartz, and biotite phenocrysts
	Amolo rhyolitic coulée	Acc	Amrc	Porphyritic with alkali feldspar, quartz, and amphibole phenocryst set in a slightly devitrified groundmass
	Pintada rhyolitic lava dome	Acc	Prlc	Porphyritic with alkali feldspar, quartz, and amphibole phenocrysts
	Chica rhyolitic coulée domes	Acc	Crdc	Porphyritic with alkali feldspar, plagioclase, and amphibole phenocrysts. Their groundmass is holohyaline partially devitrified with abundant light-gray spherulites and lithophysae
	Ahuacatla rhyolitic coulée domes	Acc	Ahrc	
	Togo rhyolitic coulée domes	Acc	Trcd	Porphyritic with alkali feldspar, plagioclase, and amphibole phenocrysts
	Canoas rhyolitic dome	Acc	Crđ	Porphyritic with alkali feldspar, quartz, and amphibole phenocrysts
	Arco rhyolitic dome	Acc	Ard	Porphyritic with scarce alkali feldspar phenocrysts
	Encimadas a rhyolitic ignimbrite	Acc	Eri	The matrix contains phenocryst of alkali feldspar, plagioclase, quartz, and amphibole
	Cabezas rhyolitic lava	Acc	Crđ	Holohyaline texture, devitrified with spherulites
	Blanco basaltic andesite scoria cones	ATVF	Bsc	Bombs are aphanitic, dark-gray color and contain plagioclase and quartz xenocrysts
	Ailitla rhyolitic coulée dome	Acc	Arcđ	Porphyritic with alkali feldspar and clinopyroxene phenocrysts
	Maguey surge fall	Acc	Msf	White-gray to greenish-gray pumice with fibrous vesicular texture and perlitic obsidian
Extra-caldera	Coatzetengo basaltic lava cones	ATVF	Colc	Porphyritic texture with olivine and plagioclase phenocrysts.
	Minilla rhyolitic coulée dome	Acc	Mrcđ	Porphyritic with alkali feldspar, plagioclase, biotite, and orthopyroxene phenocrysts
	Tetelas basaltic trachyandesite lava	ATVF	Ttal	Aphanitic with plagioclase and olivine microphenocrysts
	Tecoloquillo rhyolitic ignimbrite	Acc	Trđ	Pumice is white, fibrous and porphyritic with quartz, alkali feldspar and amphibole phenocrysts
	Moxhuite basaltic andesitic cones	ATVF	Msc	Bombs and blocks are porphyritic with plagioclase and pyroxene phenocrysts, and quartz and amphibole xenocrysts
	Coliuca basaltic scoria cones	ATVF	Clc	Bombs are dark-gray to black with aphanitic texture with plagioclase, quartz and amphibole xenocryst.
	Paila basaltic trachyandesite lava	Acc	Plc	Porphyritic with plagioclase, olivine and pyroxene phenocrysts
	The Tulimán basaltic andesite lava cone	Acc	Tlc	Aphanitic with plagioclase, amphibole and quartz xenocrysts



**Figure 3.** (A) Huistongo basaltic andesite lava flow (*Hbl*) with a blocky morphology outcropping in a road-cut. (B) View of the Aco-culco andesitic ignimbrite (*Aai*) overlaid by the Manzanito basaltic trachyandesite lava (*Mtal*). (C) Road-cut showing the Altamira rhyolitic lava flow (*Alrd*) overlaid by the distal deposits of the Tecoloquillo rhyolitic ignimbrite (*Tri*). A brownish paleosol separates these deposits. (D) Pedernal rhyolitic lava flow (*Pdl*) altered by hydrothermal activity and cut by N-S and E-W faults. (E) Quarry of the Tecajete andesitic scoria cone (*Bsc*) showing a massive fallout with lapilli-size scoria and spatter bombs. (F) Lava block sample from Section 1 (*Bsc*) with a porphyritic texture and a light-gray aphanitic enclave.

the caldera northern rim. These units were emitted towards the north of the Atotonilco scarp as coulée domes delimited by steep levées. These lavas are light-gray to pinkish-gray and cover the Puente andesitic lava domes.

The *Canoas rhyolitic dome* (*Crd*) occurs along the northern border of the caldera and at the Atotonilco gully. *Crd* has a blocky surface with a light-gray to pinkish-white color. López-Hernández et al. (2009) reported a K-Ar age on hornblende of  $1300 \pm 600$  ka for this unit. The *Crd* and *Hbl* units are intruded by an east-west basaltic dike of unknown age, which appears in the river bed of the Atotonilco gully. The dike is dark-gray with columnar jointing and an aphanitic texture.

The *Arco rhyolitic dome* (*Ard*) is exposed along the southwestern margin of the caldera. *Ard* forms an asymmetrical dome, oriented NW-SE and parallel to the Manzanito fault. This white to light-gray dome is characterized by columnar joints and a blocky lava surface. It has a mottled appearance given by abundant spherulites (up to 10 cm in diameter), lithophysae, and obsidian nodules.

The *Encimadas rhyolitic ignimbrite* (*Eri*) is widely exposed on the east-northeast sectors of the caldera margin as a moderately dissected peneplain. *Eri* is a massive, ash supported, welded ignimbrite of light-gray to white color. The matrix contains phenocryst of alkali feldspar, plagioclase, quartz, and amphibole.

*Eri* contains subrounded pink-gray aphanitic enclaves. López-Hernández et al. (2009) reported a  $^{40}\text{Ar}/^{39}\text{Ar}$  age of this rock of  $1300 \pm 200$  ka.

The *Cabezas rhyolitic lava* (*Crl*) is exposed to the western periphery of the caldera. It has a very low relief with its apex pointing to the caldera border. *Crl* is a black obsidian lava flow with angular lava fragments and planar curved faces. García-Tovar et al. (2015) reported a K-Ar age of  $1274 \pm 27$  ka for this rock.

The *Ailitla rhyolitic coulée dome* (*Arcd*) is exposed to the southeast of the caldera margin representing one of the most prominent landforms of the complex. *Arcd* is a coulée dome landform delimited by very steep levées.

The *Maguey Unit* (*Msf*) is composed of a succession of surges/fall rhyolitic pyroclastic deposits exposed to the west of the caldera margin. This unit consists of a sequence of pyroclastic flows and surge deposits with cross-bedding and parallel stratification.

The *Minilla rhyolitic coulée dome* (*Mrcd*) exposed to the northwest of the caldera rim. It is a light-gray to pinkish-gray lava flow that extends towards the west-northwest with very steep levées. It also appears with vesicular, granular-saccharoidal textures.

The *Tecoloquillo rhyolitic ignimbrite* (*Tr1*) outcrops on the southwestern rim of the caldera, where it mantles the *Pdd*, *Cal*, and *Arcd* units. *Tr1* consists of at least two light-gray non-welded, indurated, massive beds. They consist of highly friable pumice fragments and vesicular lava fragments embedded in a fine ash matrix. *Tr1* is covered by a central rhyolitic dome *Tr2* that has a blocky surface and it is composed of the same mineral association. López-Hernández et al. (2009) reported a  $^{40}\text{Ar}/^{39}\text{Ar}$  age on sanidine of  $0.8 \pm 0.1$  Ma for this unit.

The *Paila basaltic trachyandesite lava* (*Plc*) is located along the southeastern part of the caldera margin where it overlies the *Atad* and *Eri* units. It consists of dark-gray lava flows and autobreccias with vesicular blocks.

The *Tulimán basaltic andesite lava cone* (*Tlc*) occurs on the southeastern rim of the caldera where it overlies the *Hbl* and *Srl* units. *Tlc* is a massive scoria cone of red coarse to medium-grained lapilli scoria fragments and an associated lava flow. A  $^{40}\text{Ar}/^{39}\text{Ar}$  whole-rock age of *Tlc* yielded an age of  $63 \pm 9$  ka (Table 1).

### 5.5. Extra-caldera

It consists of seven units exposed around the caldera rim that are associated to the volcanism of the Apan-Tezontepec Volcanic Field.

The *Amanalco basaltic scoria cones* (*Asc*) are located at ca. 7 km to the southeast of the caldera rim. *Asc* consists of four cones (Amanalco, Huixtepec, Tecolote and Apapasco). The cones are built by massive, clast-supported and poorly sorted fallout beds. It is composed of reddish to black, medium to fine lapilli scoria and

dense blocks towards the bottom. *Asc* has a  $^{40}\text{Ar}/^{39}\text{Ar}$  whole-rock age of  $2408 \pm 58$  ka (Table 1).

The *Camelia andesitic lava flow* (*Cal*) is located 10 km to the south of the caldera. The dark-gray lava has entablature texture and a lobe-like shape with gentle slopes. *Cal* has a  $^{40}\text{Ar}/^{39}\text{Ar}$  whole-rock age of  $2033 \pm 84$  ka (Table 1).

The *Blanco basaltic andesite scoria cones* (*Bsc*) are four structures located ~6.5 km to the south of the caldera rim. The spatial distribution of these cones (Cuate, Tecajete, Blanco and Hermosa). *Bsc* are composed of massive beds (Figure 3(E–F)) with diffuse stratification and moderately to well sorted clast-supported beds. They consist of aphanitic black fine to medium-grained scoria lapilli and a few aphanitic bombs and dense blocks. *Bsc* has a  $^{40}\text{Ar}/^{39}\text{Ar}$  whole-rock age of  $1274 \pm 62$  ka (Table 1).

The *Coatzetengo basaltic lava cones* (*Colc*) are six structures located between ~4 and 7 km to the northwest of the caldera rim. *Colc* consists of five scoria cones (Buenavista, Comal, Calandria, Toronjil, and Tezontle) and the Coatzetengo half-shield volcano. All these scoria cones consist of reddish-brown to black lapilli-ash scoria and vesicular lava fragments.

The *Tetelas basaltic trachyandesite lava* (*Ttal*) occurs ca. 10 km to the south of the caldera rim. In plain view, it has a lobe-like shape with a relatively low sloping surface. The dark-gray lava appears as a single flow with columnar jointing. *Ttal* has a  $^{40}\text{Ar}/^{39}\text{Ar}$  whole-rock age of  $1060 \pm 8$  ka (Table 1).

The *Moxhuite basaltic andesitic cones* (*Msc*) are three landforms located to the east of the caldera rim. These cones have massive structures with diffuse stratification constituted by red coarse to medium-grained lapilli scoria fragments. At the base of the Moxhuite cinder cone appears abundant spatter bread-crust scoria bombs and angular blocks. A rock of the Moxhuite cinder cone has a  $^{40}\text{Ar}/^{39}\text{Ar}$  whole-rock age of  $239 \pm 34$  ka (Table 1).

The *Coliuca basaltic scoria cones* (*Clc*) are five structures located at ~7 km to the southwest of the caldera rim. They consist of four scoria cones (Coliuca, Colorado, Tezoyo, and El Conejo), and the Coyote half-shield volcano. The Coliuca cinder cone consists of scoria fallout beds composed of dark-reddish scoria lapilli and coarse ash. García-Tovar et al. (2015) reported a K-Ar age of  $190 \pm 6$  ka for the Coliuca cinder cone.

## 6. Discussion and conclusive remarks

The Aconulco caldera was defined by the presence of the Atotonilco scarp to the north, the Manzanito fault to the southwest and the venting sites on the eastern and southern parts. These structures defined an asymmetric caldera ( $18 \times 16$  km) with rhombohedral to sub-circular geometry. The distribution and stratigraphy of Ari, the occurrence of a lithic breccia, and uplifted lacustrine

deposits found inside this depression aided to define the shape of the caldera. This shape differs considerably from the nearly circular form proposed by López-Hernández et al. (2009). We have not found any evidence of a larger caldera structure (Tulancingo caldera) that would host the Acoculco caldera as suggested by López-Hernández et al. (2009).

Magmatic activity of Acoculco began ~2.7 Ma by the pressurization of the andesitic magma that disrupted the Cretaceous limestones and pre-caldera volcanics (ca. 11–3 Ma). The event produced an andesitic ignimbrite that depressurized the magma chamber causing the collapse of the magma chamber roof and the generation of syn-eruptive lithic breccias and further ignimbrite (Figure 2). The collapse formed the asymmetric caldera after which lacustrine sedimentation occurred. Early post-caldera volcanism (~2.7–2.0 Ma) was restricted to the inner part of the caldera ensuing basaltic to andesitic lava flows that were restricted inside the caldera. This magmatism bulged the central part of the caldera and uplifted the lacustrine sediments found inside the caldera rim. A period of dome extrusion emplaced the late post-caldera rhyolitic domes along the caldera rim between 2 and 1 Ma. At around 1.3 Ma, reactivation of the caldera occurred on the eastern part of the caldera generating the rhyolitic Encimadas ignimbrite. Another explosive event occurred ~0.8 Ma at the southwestern margin of the caldera producing the Tecoloquillo rhyolitic ignimbrite and its summit dome. The last two events link to the evolution of the caldera emitted the Tulliman lava cone (0.063 ka), and the la Paila scoria cone nearby the caldera rim. Extra-caldera volcanism of the Apan-Tezontepec Volcanic Field (~3.00 to ~0.19 Ma) emplaced basaltic scoria cones, associated lava flows, and a few half-shield volcanoes. These mafic volcanism were coeval with the calc-alkaline volcanism in the Acoculco region that ended with a more complex evolution through time (Sosa-Ceballos et al., 2018).

These authors classified the Miocene rocks of the TMVB, the pre-caldera, and those associated with the different stages of the caldera evolution as subduction related calc-alkaline magmas (e.g. enriched in mobile elements, Nb-Ta negative anomalies, Pb positive anomaly). These authors also concluded that after the caldera collapse peralkaline magmas were able to rise through new plumbing system mixing with the calc-alkaline magmas to generate the post-caldera volcanism with negligible assimilation. These peralkaline magmas were able to reactive venting sites along the ring fault producing the rhyolitic Encimadas and Tecoloquillo ignimbrites.

## Software

This map was produced by using ArcMap 10.2 and ERDAS imagine 9.1 programs.

## Acknowledgements

We thank S. Cardona for their technical support during laboratory analyses. We thank the reviewers C. Orton, F. Di Traglia, B. Coira, K. Turner, J. Abraham, K. Turner, L. Ferrari, G. Carrasco, and J. Moles for their valuable comments and suggestions provided.

## Disclosure statement

No potential conflict of interest was reported by the authors.

## Funding

This study was funded by Grant 207032 of the Centro Mexicano de Innovación en Energía Geotérmica (CeMIE Geo) project P15 to J.L. Macías. JM is grateful for the MECD (PRX16/00056) grant.

## ORCID

José Luis Macías  <http://orcid.org/0000-0002-2494-9849>

## References

- Benowitz, J. A., Layer, P. W., & Vanlaningham, S. (2014). Persistent long-term (c. 24 Ma) exhumation in the Eastern Alaska Range constrained by stacked thermochronology. *Geological Society, London, Special Publications*, 378, 225–243.
- Campos-Enríquez, J. O., Alatraste-Vilchis, D. R., Huizar-Álvarez, R., Marín-Campos, R., & Alatorre-Zamora, M. A. (2003). Subsurface structure of the Tecocomulco sub-basin (northeastern Mexico basin), and its relationship to regional tectonics. *Geofísica Internacional*, 42, 3–24.
- De la Cruz-Martínez, V., & Castillo-Hernández, D. (1986). Geología de la zona geotérmica de la caldera de Acoculco, Puebla. *Geotermia, Revista Mexicana de Geoenergía*, 2, 245–254.
- Demant, A. (1978). Características del Eje Neovolcánico Transmexicano y sus problemas de 604 interpretación. *Revista Mexicana de Ciencias Geológicas*, 2, 172–187.
- García-Palomo, A., Macías, J. L., Jiménez, A., Tolson, G., Mena, M., Sánchez-Núñez, J. M., ... Lermo-Samaniego, J. (2017). NW-SE Pliocene-Quaternary extension in the Apan-Acoculco region, eastern Trans-Mexican Volcanic Belt. *Journal of Volcanology and Geothermal Research*, 349, 240–255.
- García-Palomo, A., Macías, J. L., Tolson, G., Valdez, G., & Mora, J. C. (2002). Volcanic stratigraphy and geological evolution of the Apan región, east-central sector of the Trans-Mexican Volcanic Belt. *Geofísica Internacional*, 41, 133–150.
- García-Tovar, G. P., Martínez-Serrano, R. G., Solé, J., Correa-Tello, J. C., Núñez-Castillo, E. Y., Guillou, H., & Monroy-Rodríguez, E. (2015). Geología, geocronología y geoquímica del vulcanismo Plio-Cuaternario del Campo Volcánico Apan-Tecocomulco, Faja Volcánica Trans-Mexicana. *Revista Mexicana de Ciencias Geológicas*, 32, 100–122.
- Huizar-Álvarez, R., Campos-Enríquez, J. O., Lermo-Samaniego, J., Delgado-Rodríguez, O., & Huidobro-González, A. (1997). Geophysical and hydrogeological characterization of the sub-basins of Apan and Tochac (Mexico Basin). *Geofísica Internacional*, 36, 217–234.

- Lermo, J., Antayhua, Y., Bernal, I., Venegas, S., & Arredondo, J. (2009). Monitoreo sísmico en la zona geotérmica de Acapulco, Pue., México. *Geothermia*, 22, 40–58.
- Lopez-Hernandez, A., & Castillo-Hernandez, D. (1997). Exploratory drilling at Acapulco, Puebla, Mexico: a hydrothermal system with only nonthermal manifestations (Report No. CONF-971048--). United States: Geothermal Resources Council, Davis, CA.
- López-Hernández, A., García-Estrada, G., Aguirre-Díaz, G., González-Partida, E., Palma-Guzmán, H., & Quijano-León, J. (2009). Hydrothermal activity in the Tulancingo–Acapulco caldera complex, central Mexico: Exploratory studies. *Geothermics*, 38, 279–293.
- López-Hernández, A., & Martínez, E. I. (1996). Evaluación volcanológica y estructural de la zona geotérmica de Acapulco, Puebla, y su relación con la anomalía termal detectada en el pozo EAC-1 (Internal Report OGL-AC-11/96). México: CFE-GPG.
- Mooser, F., & Ramírez, M. T. (1987). Faja Volcánica Transmexicana: Morfoestructura, tectónica y vulcanotectónica. *Boletín de la Sociedad Geológica Mexicana*, 48, 75–80.
- Ryan, W. B. F., Carbotte, S. M., Coplan, J. O., Óhara, S., Melkonian, A., Arko, R., ... Zensky, R. (2009). Global multi-resolution topography synthesis. *Geochemistry, Geophysics, Geosystems*, 10, 1–9.
- Sosa-Ceballos, G., Macías, J. L., Avellán, D. R., Salazar-Hermenegildo, N., & Boijseuneau-López, M. E. (2018). The Acapulco Caldera complex magmas: Genesis, evolution and relation with the Acapulco geothermal system. *Journal of Volcanology and Geothermal Research*, 358, 288–306.
- Steiger, R. H., & Jäger, E. (1977). Subcommittee on geochronology: Convention on the use of decay constants in geo- and cosmochronology. *Earth Planet. Sci. Lett.*, 36, 359–362.
- Urrutia-Fucugauchi, J., & Flores-Ruiz, J. (1996). Bouguer gravity anomalies and regional crustal structure in central Mexico. *International Geology Review*, 38, 176–194.
- Viggiano-Guerra, J. C., Flores-Armenta, M., & Ramírez-Silva, G. R. (2011). Evolución del sistema geotérmico de Acapulco, Pue., México: un estudio con base en estudios petrográficos del pozo EAC-2 y en otras consideraciones. *Geothermia*, 24, 14–24.